Parallel but distinct adaptive routes in the budding and fission yeasts after 10,000 generations of experimental evolution

Authors: Arnaud N'Guessan[1], Vivian Wang[1], Joao Ascensao[2], Christopher W. Bakerlee[2,3,4], Evgenia Belousova[2], Greta Brenna[2], Megan E. Dillingham[5], Thomas Dupic[2], Shreyas Gopalakrishnan[2], Juhee Goyal[2,6], Misha Gupta[2], Caroline Holmes[2], Parris T. Humphrey[2,4], Tanush Jagdish[2,4,5], Elizabeth R. Jerison[2,7,8], Milo S. Johnson[2,4], Katya Kosheleva[2,8], Katherine R. Lawrence[2,4,9], Jiseon Min[2,3,4,6], Alief Moulana[2], Shreyas Pai[5], Angela M. Phillips[2], Julia C. Piper[8,10], Alexandra Poret[2,8,11], Ramya Purkanti[2,12], Artur Rego-Costa[2], Tatiana Ruiz-Bedoya[2], Cecilia Trivellin[2], Michael J. McDonald[2,13], Michael M. Desai[2,4,8], Alex N. Nguyen Ba[1,14]

1. Department of Cell and Systems Biology, University of Toronto, Ramsay Wright Laboratories, 25 Harbord St, M5S 3G5, Toronto, Ontario, Canada.
2. Department of Organismic and Evolutionary Biology, Harvard University, Cambridge MA 02138, USA
3. Department of Molecular and Cellular Biology, Harvard University, Cambridge, United States.
4. NSF-Simons Center for Mathematical and Statistical Analysis of Biology, Harvard University, Cambridge, United States.
5. Graduate Program in Systems, Synthetic, and Quantitative Biology, Harvard University, Cambridge, United States
6. John A Paulson School of Engineering and Applied Sciences, Harvard University, Cambridge, United States.
7. Department of Applied Physics, Stanford University, Stanford, United States.
8. Department of Physics, Harvard University, Cambridge MA 02138, USA
9. Department of Physics, Massachusetts Institute of Technology, Cambridge, United States.
10. AeroLabs, Aeronaut Brewing Co, Somerville, United States.
11. Graduate Program in Biophysics, Harvard University, Cambridge, MA, USA
12. The Max Planck Institute of Molecular Cell Biology and Genetics, Dresden, Germany.
13. School of Biological Sciences, Monash University, Clayton, Victoria, Australia
14. Department of Biology, University of Toronto at Mississauga, 3359 Mississauga Rd, L5L 1C6, Mississauga, Ontario, Canada

ABSTRACT

Quantitative genetics approaches designed to understand the evolution of traits have helped improve our understanding of the genetic basis of adaptation. However, they often overlook crucial aspects of adaptation, including the long-term temporal evolutionary dynamics, the predictability of evolutionary outcomes, the influence of past evolution on future evolutionary trajectories (contingency), and the extent and diversity of molecular mechanisms underlying adaptation. Experimental evolution has been a useful tool to answer these questions, but extracting fundamental principles and predictive features of evolutionary outcomes from these datasets remains challenging due to the large number of covariates and confounding effects, such as differences in experimental setups, species lifestyle, gene content, and evolution rate. Here, we sought to circumvent these challenges by comparing distant yeast species with similar evolutionary

features but different evolutionary history and genome architecture, i.e. *Saccharomyces cerevisiae* and *Schizosaccharomyces pombe*. We evolved 10 populations of the fission yeast for 10,000 generations in the same conditions as a pre-existing budding yeast dataset, i.e. high-sugar media and hypoxic conditions, allowing us to observe repeatable evolutionary outcomes within species but diverse molecular mechanisms and targets of adaptation across species. Most of the *S. pombe* evolved populations exhibited adaptations to hypoxic stress (HS) at the expense of increased sensitivity to oxidative stress (OS). This trade-off has not previously been observed in *S. cerevisiae* evolved populations or wild *Kluyveromyces lactis,* but is seen in *Schizosaccharomyces japonicus* and clinically relevant populations such as some cancer cells, indicating that parallelism is pervasive in the tree of life and that mechanisms of adaptation can be shared among closely related or distant species. Despite similar gene content and identical environments, recurrent adaptations across *S. pombe* populations involved different genes than in *S. cerevisiae* and were mostly detectable at the transcriptomic level. This suggests that trans-regulatory effects may play an important role in adaptation on short evolutionary timescales and that differences in evolutionary outcomes between these species may be attributed to contingency.

INTRODUCTION

Long-term experimental evolution has highlighted the predictability of high-level features of evolution like fitness trajectories[1–6]. While fitness gain follows a fairly reproducible pattern of declining adaptability, the exact mutations or the sequence in which they occur are typically not predictable. Nevertheless, experimental evolution done in large replication with the budding yeast *Saccharomyces cerevisiae* has revealed extensive parallelism at the gene or pathway level[3,7,8], even across strains that differed by thousands of polymorphisms[9]. These general patterns of reproducibility during experimental evolution are also seen in different organisms. For instance, during the *Escherichia coli* Long-Term Experimental Evolution (LTEE), half of the populations evolved a mutator phenotype and quasi-stable lineage coexistence emerged in 75% of the populations[4]. Further, substantial parallelism at the gene level can also be observed throughout the 12 populations over (now greater than) 60,000 generations[4].

Unsurprisingly, the molecular targets of selection during these experiments differ substantially between *S. cerevisiae* and *E. coli*. Likewise, comparing microbial laboratory evolution to experimental evolution done in *Caenorhabditis elegans* and *Drosophila melanogaster* does not reveal universal targets of adaptation[10,11]. Notwithstanding their vastly different gene content and cellular form, part of the reason for these differences in molecular adaptation is the different selection environments between experiments (the LTEE was done in M9 minimal media, while yeast was done in YPD rich media or in synthetic dextrose complete media). However, another more interesting hypothesis for these differences relates to the role of evolutionary contingency in shaping the dynamics and targets of selection.

Contingency is the product of past evolution, whereby epistasis and genome structures can strongly influence future adaptive potential[1,12,13]. Thus, species can be constrained to alternative adaptive paths, which can lead to profoundly different molecular signatures of evolution. Contingency has been explored in the context of strains with different gene deletions[13–16] and has even been observed in experimental evolution. For instance, across the 12 *E. coli* populations evolving in the same conditions during the LTEE, one population developed the ability to grow aerobically on citrate, a rare phenotype in this species resulting from a rare genome rearrangement. This phenotype is far more readily evolvable within that population after this rearrangement[17]. Further, while half of the LTEE populations evolved a mutator phenotype, and 75% evolved stable lineage coexistence, these phenomena are not observed in *S. cerevisiae* laboratory evolution experiments in standard rich media or in minimal media, despite being entirely capable of achieving these observations through genetic engineering[18].

While studying evolution using very distinct organisms has provided important insights into general features of evolutionary dynamics, it has made it difficult to discern the effect of life history from other idiosyncrasies on the molecular targets of selection. Would we find the same targets of selection, or would we observe selection on the same molecular mechanisms if we had evolved a species with substantially similar gene contents to that of *E. coli* or *S. cerevisiae*? The difficulty in answering this question is also reinforced by the wide variety of mechanisms of rapid adaptation revealed by long-term evolution studies, e.g. hybridization, selection on standing variation, cross-feeding interactions or phenotypic plasticity involving behavioral or transcriptomic changes[11].

Evaluating the impact of differences between such species on quantitative trait evolution could improve our understanding of the processes involved in adaptation and their contribution in trait diversity.

One way to address how much genome and life-trait history might influence long-term adaptation is through the yeast subphylum as it exhibits immense trait diversity and is as genetically diverse as the animal kingdom[19,20], but species within have a comparable number of genes, and share many genes and metabolic pathways such that most species can grow in the same media. As an example, *S. cerevisiae* and *Schizosaccharomyces pombe* share about 4,500 genes (out of approximately 6,000), but are so diverged that their genomes show no synteny. Evolutionarily, they have similar spontaneous mutation rates and were both domesticated for their ability to ferment. Their similarities likely end here. Some notable differences are that *S. pombe* is naturally a haploid in the wild[21,22], while *S. cerevisiae* is usually found as a diploid[23,24]. This could affect the effectiveness of selection because mutations can be recessive in diploids. Therefore, the extant genome might have 'footprints' of this through the accumulation of genetic load in *S. cerevisiae*[3,25]. Supporting this, heterosis has been observed in yeast from crosses of wild budding yeast strains[26,27]. Further, *S. cerevisiae* is within the clade of yeasts that have undergone the so-called 'whole-genome duplication event', which is thought to have profoundly shaped their metabolism due to functional divergence in paralogous gene copies[28]. Another major difference is that *S. pombe* is petite-negative, while *S. cerevisiae* is petite-positive, highlighting a rare ability of budding yeast [29–31]. Thus, domestication, competition with other microorganisms, and exploration of poorly oxygenated niches might have led *S. cerevisiae*[32,33]. Therefore, their different life cycles and evolutionary histories could lead them to different evolutionary outcomes even if presently evolved in the same environment.

Hints on the effects of contrasting life and evolutionary histories on evolutionary signatures emerge when comparing the molecular processes that were under selection and could potentially allow for the prediction of molecular evolution that may occur during experimental evolution. For example, *S. cerevisiae* gene content variation across strains is more frequent than in *S. pombe*, and loss-of-function (LOF) mutations, such as nonsense mutations and frameshift deletions, tend to be recurrently fixed across populations[34]. The rate of copy number variants (CNV) is also higher in the budding yeast sub-telomeric regions and can contribute to its adaptation[34]. Additionally, although *S. pombe* has a similar substitution rate to the budding yeast, it has a higher indel mutation rate with a bias toward insertions[35]. Previous genomic analyses also showed that 43% of *S. pombe* genes have introns compared to 5% in *S. cerevisiae* and upstream intergenic regions are larger in the former[36]. The difference in extent of non-coding regions is also present at the whole-genome level: annotated coding regions span around 70% of *S. cerevisiae* genome compared to 60% for *S. pombe*[37–39]. It is currently unknown if this implies that *S. pombe* would preferably adapt through regulatory changes while *S. cerevisiae* would do so through gene content changes and mutations in protein-coding genes. However, the mutations in the non-coding regions of *S. pombe* are known to be involved in transcription regulation and should affect trait evolution and adaptation[40]. Thus, comparing the evolutionary processes and targets of adaptation in *S. cerevisiae* and *S. pombe* through experimental evolution could help highlight factors explaining differences in evolutionary outcomes across and within species.

To address the gap in understanding how species with similar gene content, but different life histories, might evolve in the same environment, we undertook a laboratory evolution experiment where we founded about 16 populations each of 5 different budding yeast species, as well as the *S. pombe* fission yeast. Here, we describe the dynamics and molecular evolution of the fission yeast populations over the first 10,000 generations. Fission yeast is considered the outgroup of this set of species, and so it serves as a useful anchor for expectations within our chosen fungal phylum. We analyze the mutational spectrum, the molecular evolutionary dynamics, and identify, through pathway enrichment analysis and whole transcriptome sequencing, a case of parallel evolution where *S. pombe* populations have rewired their central carbon metabolism to reduce dependency on oxygen, which mirrors similar events in wild *S. pombe* populations and in related *Schizosaccharomyces*[30,33,33,41,42].

RESULTS

Contrasting fitness gain of fission yeast during 10,000 generations of evolution

To compare the evolution processes contributing to adaptation and selection targets between *S. pombe* and *S. cerevisiae*, we founded 15 *S. pombe* populations and performed experimental evolution for 10,000 generations, collecting and freezing samples approximately every 70 generations in 20% glycerol (**Methods; Figure 1**). The populations were all founded from single colonies of the same 972h- *S. pombe* laboratory strain and serially propagated in batch culture in one well of a lidded, unshaken flat-bottom 96-well plate in rich media at 30°C with a daily $1{:}2^{10}$ dilution. 5 populations were lost during the first 10,000 generations of evolution, due to contamination or mechanical pipetting errors. Because of the plate lidding and the absence of shaking, these conditions correspond to a high-sugar hypoxic environment, and are identical to our previous study that analyzed 10,000 generations of evolution for *S. cerevisiae* populations[3].

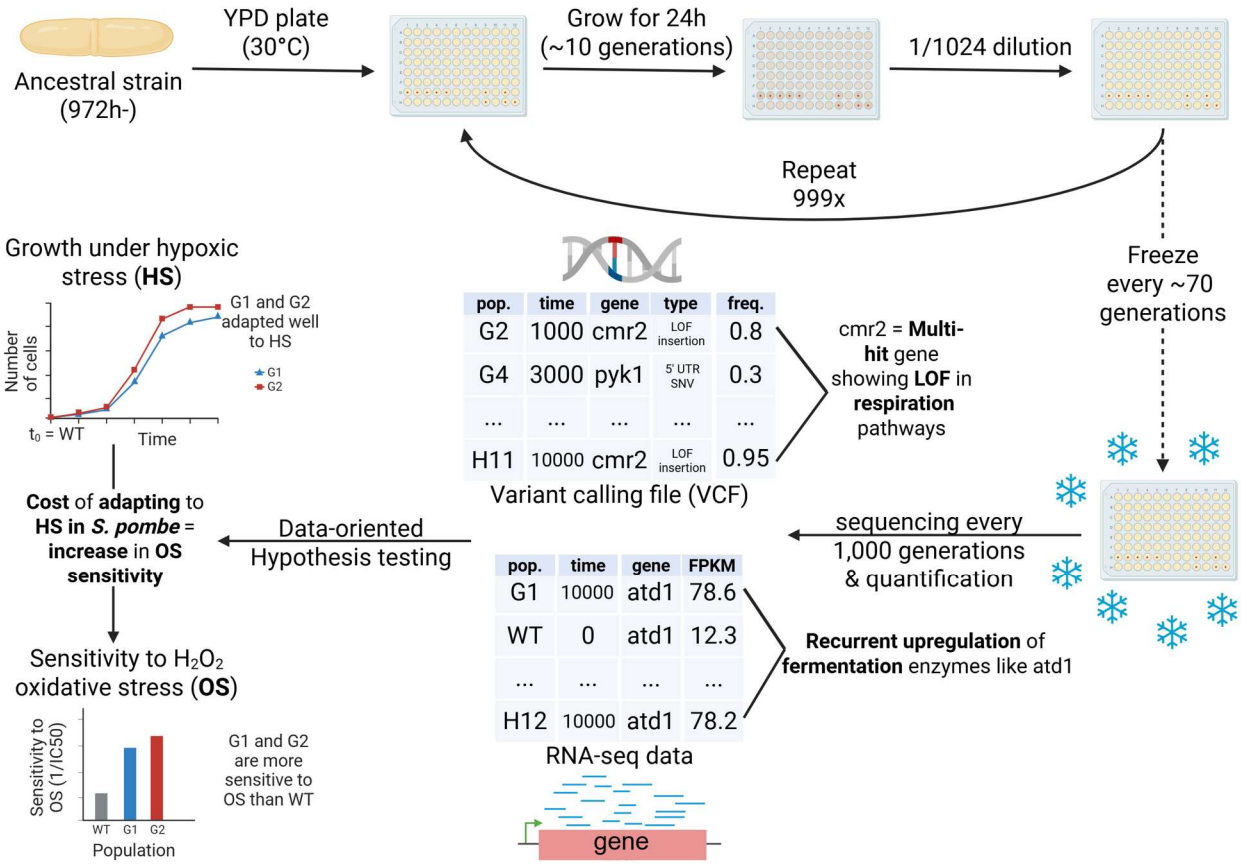

Figure 1 Experimental approach. We evolved 15 *S. pombe* populations at 30°C in sealed YPD 96-well plates for 10,000 generations, collecting and freezing samples approximately every 70 generations in 20% glycerol at -80 °C and sequenced them every 1,000 generations. These populations were part of a larger experimental evolution project, which explains why they occupy two rows of the 96-well plates and were examined regularly for contamination (**Methods**). Because the experimental conditions yielded a doubling rate of 10 generations per day, we performed a 1/1024 serial dilution every day ($1/2^{10}$), which can be done by two consecutive 1:32 dilutions with 96-well plates. This yielded ~100 time points or samples from which we sequenced DNA to identify variants and RNA at the initial (WT) and final time points to quantify gene expression changes. To find targets of selection at the genomic levels, we identified multi-hit genes, i.e. the genes that were recurrently hit by fixed mutations (frequency >= 75%) that are not synonymous (indels, missense or nonsense) in multiple populations. At the transcriptomic level, we identified genes that were frequently differentially expressed across evolved populations. These data allowed us to generate hypotheses about adaptation in the 10 populations surviving, i.e. G1-G5, G9, H9 and H11-12, which we tested experimentally.

To determine whether the evolved populations adapted to these conditions, we measured the fitness at the initial and final time points. We serially propagated each population and the ancestral strain separately in a mixture with a *S. cerevisiae* reference strain expressing green fluorescent protein (GFP) for 3 days. We used a flow cytometer to measure the frequency of the dark *S. pombe* populations and the green *S. cerevisiae* strain daily, and assessed fitness based on changes in frequency (**Equation 1 in Methods**). The evolved populations are all fitter than the

ancestral strain (**Supplementary Figure 1**) as observed in other experimental evolution studies[3,6]. However, the fitness gains of the *S. pombe* lineages after 10,000 generations of evolution are significantly smaller than those of *S. cerevisiae*'s haploid populations in a similar rich-media hypoxic environment (**Supplementary Figure 1**). This slower rate of fitness gain is not due to *S. pombe* being 'pre-adapted' to this environment, as the ancestor *S. cerevisiae* strain used in a previous study is much fitter than the ancestor *S. pombe* strain used here. We presume that this is the result of *S. cerevisiae* having a higher glycolytic and fermentation rates, and can more readily adapt to the experimental conditions through a more diversified set of stress response pathways as a result of having explored many anaerobic niches throughout its evolutionary history[30,32,33,43]. *S. pombe*, on the other hand, is a poor fermenter in anaerobic conditions[30] and has a less robust hypoxic stress response[44]. Together, these factors may partly explain the differences in adaptation rate in the same environmental conditions, as each species might evolve through different adaptation strategies that have different associated costs.

Differences in the genome architecture partially explain the different mutation spectra of *S. pombe* and *S. cerevisiae*

To uncover potential differences in adaptation strategies between the two species and the molecular mechanisms underlying them in the evolved populations, we performed whole-population, whole-genome sequencing every 1,000 generations on the 10 *S. pombe* populations. We successfully grew cells from 93 out of the 100 corresponding stored samples and sequenced these time points using Illumina NovaSeq paired-end sequencing (mean coverage ~40X). The remaining 7 time points were presumably lost during storage and were not associated to any specific population or particular archival date. We then called single-nucleotide variants (SNVs) and indels using Varscan2.4.6[45]. Because contamination, sequencing errors and low-complexity regions can introduce variant calling errors, we applied some filters to the called variants [46,47] while leveraging the time series for call consistency (**Methods**).

To validate the accuracy of the called variants, we measured the substitution rates and fixed indel bias, e.g., the fixed insertion-to-deletion ratios, in each *S. pombe* population. We measured a fixed insertion-to-deletion ratio ranging from 2.11 to 6.33 (median = 4.43, μ= 4.32, σ= 1.22), which is consistent with the insertion preference observed in previous *S. pombe* genomic analyses [35]. This preference for insertion is partly the result of the fixation of insertions in the populations (**Supplementary Figure 2**). As for the substitution rate, we measured an average of 1.91E-10 substitutions per site per generation (median = 1.72E-10, σ= 6.76E-11), which is similar to results from mutation accumulation experiments in *S. pombe* (2.00E-10 in Farlow et al. 2015) and within the range of *S. cerevisiae*'s substitution rate estimates (1.67 ± 0.04E-10 in Zhu et al. 2014 and 3.30± 0.80E-10 in Lynch et al. 2008)[35,48,49].

Although both species mutate at a similar rate, their genome architectures differ. *S. cerevisiae* is a domesticated post-WGD yeast species, contrarily to *S. pombe* [50–53]. Furthermore, the extent of coding regions in *S. pombe*'s genome (~60%) is smaller than in *S. cerevisiae* (~70%) [32,35,54,55]. Under a null model of evolution in which all loci have the same chance of being hit by

substitutions, the differences in the mutation spectra of these species should reflect the differences in genome architecture. Deviations from this expectation would suggest the presence of selection in certain loci and a preference for specific types of mutations. Thus, we compared the frequency of different variants observed in the 10 *S. pombe* haploid populations to the one observed in *S. cerevisiae* haploid populations' experimental evolution[3] (**Figure 2A**).

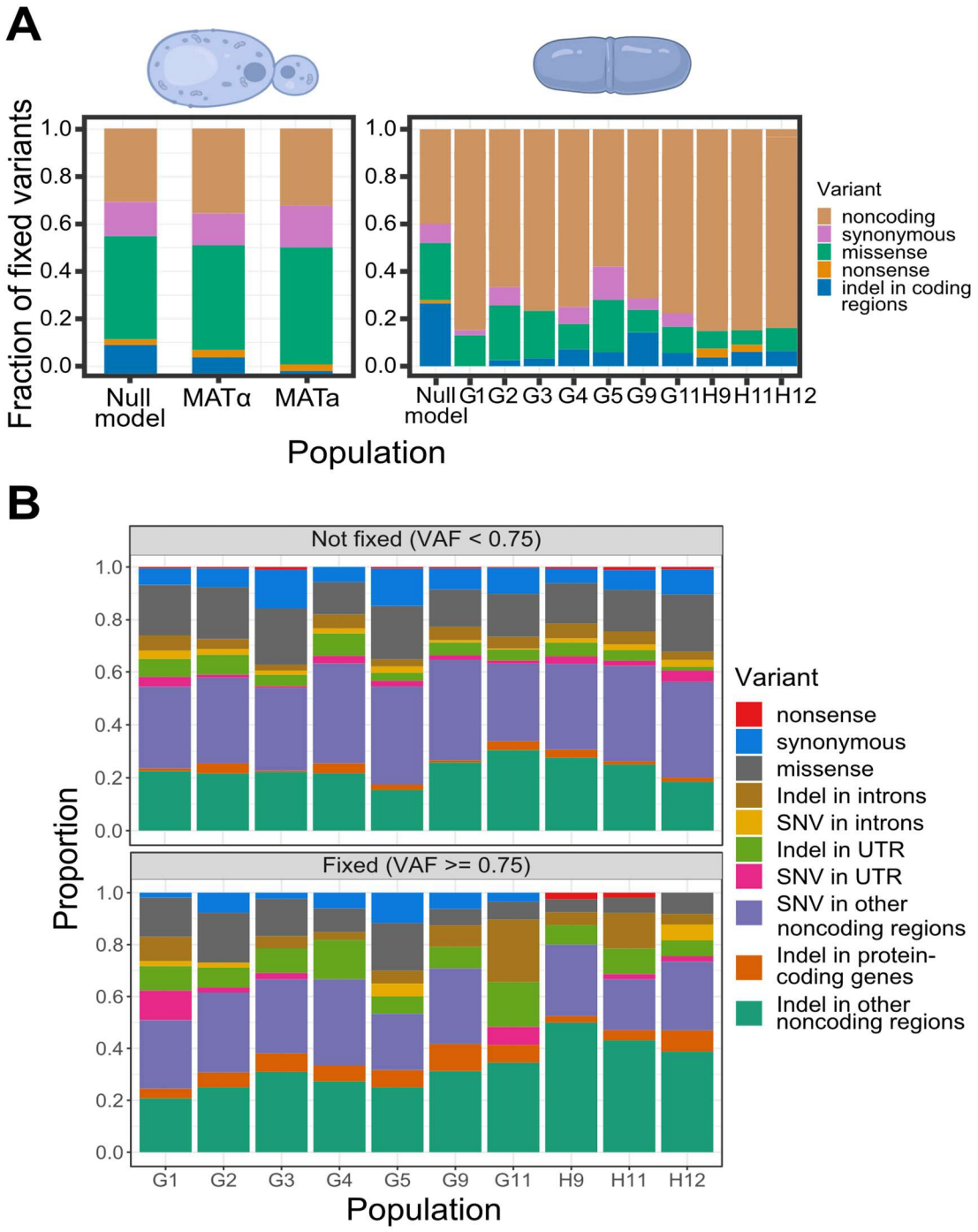

Figure 2 Comparison of the fixed variant spectra between the budding and the fission yeasts and the fixation bias in *S. pombe* evolved populations. A) The fixed variant (allele frequency

>= 75%) spectrum in *S. cerevisiae*'s haploid populations after 10,000 generations of experimental evolution (left, data from Johnson et al. 2021) compared to *S. pombe*'s (right). The experimental evolution protocol is the same for both species and is described in Johnson et al. 2021[3]. The null model is obtained by calculating the expected number of fixed variants in each category based on the species' evolution rate, genome size, genome architecture, and the proportion of single-nucleotide mutations derived from the genetic code and associated with a specific category of protein-coding region mutations (**Equations 2 and 3 in Methods**). B) The upper part of this panel represents non-fixed variants, while the bottom part represents the fixed variants in each of the 10 evolved *S. pombe* populations.

The fixation of variants in the noncoding regions of *S. pombe* is higher than expected by the null model, suggesting the predominance of positive selection in noncoding regions or purifying selection in coding regions. The fission yeast populations mainly evolved through mutations in non-coding regions with a bias toward fixing indels and not fixing coding regions SNVs (**Figure 2B**), which is different than what has been reported for the budding yeast[3]. To test if the stronger fixation bias of indels in non-coding regions compared to protein-coding genes reflects a signal of purifying selection in protein-coding genes, we compared the indel rate, i.e., the number of indels per kb, based on whether the indel locus is coding or non-coding and whether the indel changes the DNA reading frame or not (**Supplementary Figure 3**). In protein-coding genes, most indels are either short (1 or 2 bp) due to their higher likelihood (**Supplementary Figure 3**) or do not cause a frameshift in the gene, in contrast to indels in non-coding regions. This is similar to the observed frequencies of polymorphisms in humans and budding yeast[56], suggesting the presence of purifying selection on frameshifting indels in protein-coding genes. Altogether, these results show that the differences in the mutation spectra of *S. cerevisiae* and *S. pombe* are only partially explained by their genome architectures, revealing signatures of selection in both coding and non-coding regions.

The genomic targets of adaptation in *S. pombe* are genes involved in the response to hypoxic and oxidative stresses

Although the *S. pombe* mutation spectrum revealed a signal of purifying selection in protein-coding genes, we cannot exclude the presence of loci evolving under positive selection. However, we may expect the targets of adaptation to vary between fission and budding yeasts due to differences in their evolutionary histories and genetic architectures. To detect such loci in 205 *S. cerevisiae* populations, Johnson et al. (2021) looked for signals of convergent evolution. More precisely, they defined a "hit" as a fixed variant that is not synonymous (missense, nonsense and indels), and a multi-hit gene as a gene having hits in multiple populations. This enabled the identification of 1,092 genes with hits in at least 3 out of 205 populations. Among these genes, they identified a set of 189 genes with hits in at least 6 populations that were enriched in functions related to the adenine biosynthesis pathway, the mating pathway, and negative regulators of the Ras pathway. These signals of parallelism at the levels of biosynthetic and signaling pathways were driven by LOF mutations, which were primarily frameshift deletions and nonsense mutations.

Using the same approach with a minimum threshold of 2 out of 10 populations in which a gene has a hit, we identified 19 multi-hit genes (**Table 1**).

Gene symbol (systematic ID)	Function(s) (biological process)	Link with the response to HS and OS	Number of popula-tions with a gene hit	Loss-of-function hits (Effect)
bmc1 (SPBC2A9.10)	Bin3 family RNA methyltransferase (snRNA metabolic process)	Not found	2	-Frameshift insertion chrII_T2965030+A in the populations G1 and G3 (Truncation of 14 out of 269 residues)
bop1 (SPAP32A8.03c)	ubiquitin-protein ligase E3 (protein degradation)	-Ubiquitin-dependent protein degradation is ATP-dependent[57,58] and could be reduced under HS -Negative genetic interaction with Pap1 (transcription factor involved in OS response and binding Prr1)[59]	2	-Frameshift insertion chrI_T3408209+G in the populations G11 and H12 (Truncation of 475 out of 514 residues)
clg1 (SPBC1D7.03)	Cyclin-like protein involved in autophagy (signaling, molecular activity regulation and autophagy)	-In *S. pombe*, *clg1* regulates autophagy[60] -Autophagy plays an important role in the response to HS and OS by recycling biomolecules and removing	2	Not found

		damaged cell components[61,62]		
cmr2 (SPAC56F8.02)	acetyl-CoA biosynthesis (respiration)	-Acteyl-CoA is involved in the first step of the TCA cycle (respiration)	2	-Nonsense SNP chrI_C1128193T in the population H11 (Truncation of 174 out of 1518 residues in the response regulator receiver domain and disordered regions in C-terminal)
ctf18 (SPBC902.02c)	Ctf18 RFC-like complex subunit Ctf18 (DNA replication)	-Upregulated under HS[61]	4	Not found
dep1 (SPBC21C3.02c)	Rpd3L histone deacetylase complex subunit (chromatin organization and transcription regulation)	-Upregulated under HS[61] -*dep1Δ* strain is more sensitive to hydrogen peroxide[63]	2	Not found
fet4 (SPBP26C9.03c)	plasma membrane iron/zinc ion transmembrane transporter (inorganic ion homeostasis and transmembrane transport)	-Iron transport is important under HS[64] (heme metabolism and electron transport chain with limited oxygen)	2	Not found
fhn1 (SPBC1685.13)	Eisosome assembly protein (membrane organization)	-Upregulated during the response to hydrogen peroxide[65]	3	Not found
iss9 (SPBC2A9.11c)	SAC3/GANP/THP3 family protein (transcription or RNA surveillance)	Not found	2	-Frameshift insertion chrII_C2966290+T in the populations G1 and G5 (Truncation

				of 315 out of 396 residues)
pfl2 (SPAPB15E9.01c)	cell surface glycoprotein, flocculin Pfl2 (cell adhesion)	Flocculation and adhesion enhance survival by protecting against stressful conditions[66,67]	3	Not found
pfl5 (SPBC1289.15)	cell surface glycoprotein, flocculin Pfl5 (cell adhesion)	Flocculation and adhesion enhance survival by protecting against stressful conditions[66,67]	3	-Frameshift insertion chrII_A4423656+AAACT and deletion chrII_T4423650-GTTGG in the populations G2 and H12 (Truncation of 518 and 528 out of 1284 residues, respectively)
pof15 (SPAPB1A10.14)	Ubiquitin complex adaptor; F-box protein (protein degradation)	-Upregulated under HS[61] -Upregulated during the response to an oxidative stress[68] -Ubiquitin-dependent protein degradation is ATP-dependent[57,58]	2	-Frameshift deletion chrI_T1891186-ACCGATTC in the populations G5 and H12 (Truncation of 135 out of 244 residues)
pqr1 (SPAC6B12.07c)	ubiquitin-protein ligase E3, phosphate quantity regulator Pqr1/Spx1 (protein degradation and transmembrane transport)	-Upregulated during the response to hydrogen peroxide[65] -Ubiquitin-dependent protein degradation is	3	Not found

		ATP-dependent[57,58]		
prr1 (SPAC8C9.14)	stress-responsive DNA-binding transcription factor Prr1 (transcription regulation and response to oxidative stress)	-*prr1* regulates *ctt1*, *srx1*, *trr1* during the cellular response to OS[69,70]	2	-Frameshift insertion chrI_C3666021+G in the population H11 (Truncation of 517 out of 540 residues)
pyk1 (SPAC4H3.10c)	pyruvate kinase (carbohydrate metabolic process)	-Involved in glycolysis (last step) and respiration -Upregulated under HS[61]	5	Not found
pzh1 (SPAC57A7.08)	serine/threonine protein phosphatase (signaling)	-*pzh1* modulates the response to OS[71] -Upregulated under HS[61]	2	Not found
rpp1 (SPAC3A12.04c)	RNase P and RNase MRP subunit p30 (ribosome biogenesis and tRNA metabolic process)	Not found (Gene knockout is not viable)	2	Not found
seb1 (SPAC222.09)	poly(A)site selection protein (mRNA metabolic process and snoRNA metabolic process)	Not found (Gene knockout is not viable)	2	Not found
ubp9 (SPBC1703.12)	ubiquitin C-terminal hydrolase Ubp9 (protein degradation and vesicle-mediated transport)	-*ubp9Δ* strain is more sensitive to hydrogen peroxide[63] -Ubiquitin-dependent protein	2	-Frameshift insertion chrII_T2937277+A in the populations G3 and G9 (Truncation of 265 out of 586 residues)

		degradation is ATP-dependent[57,58]		

Table 1 Multi-hit genes and their LOF mutations. The gene annotations are based on Pombase data[38].

The presence of hits in multi-hit genes was more recurrent than expected under neutral evolution[72] (Wilcoxon rank sum p-value < 0.05; **Supplementary Figure 4**). This signal of positive selection is also consistent with the fixation of these hits (**Figure 3**).

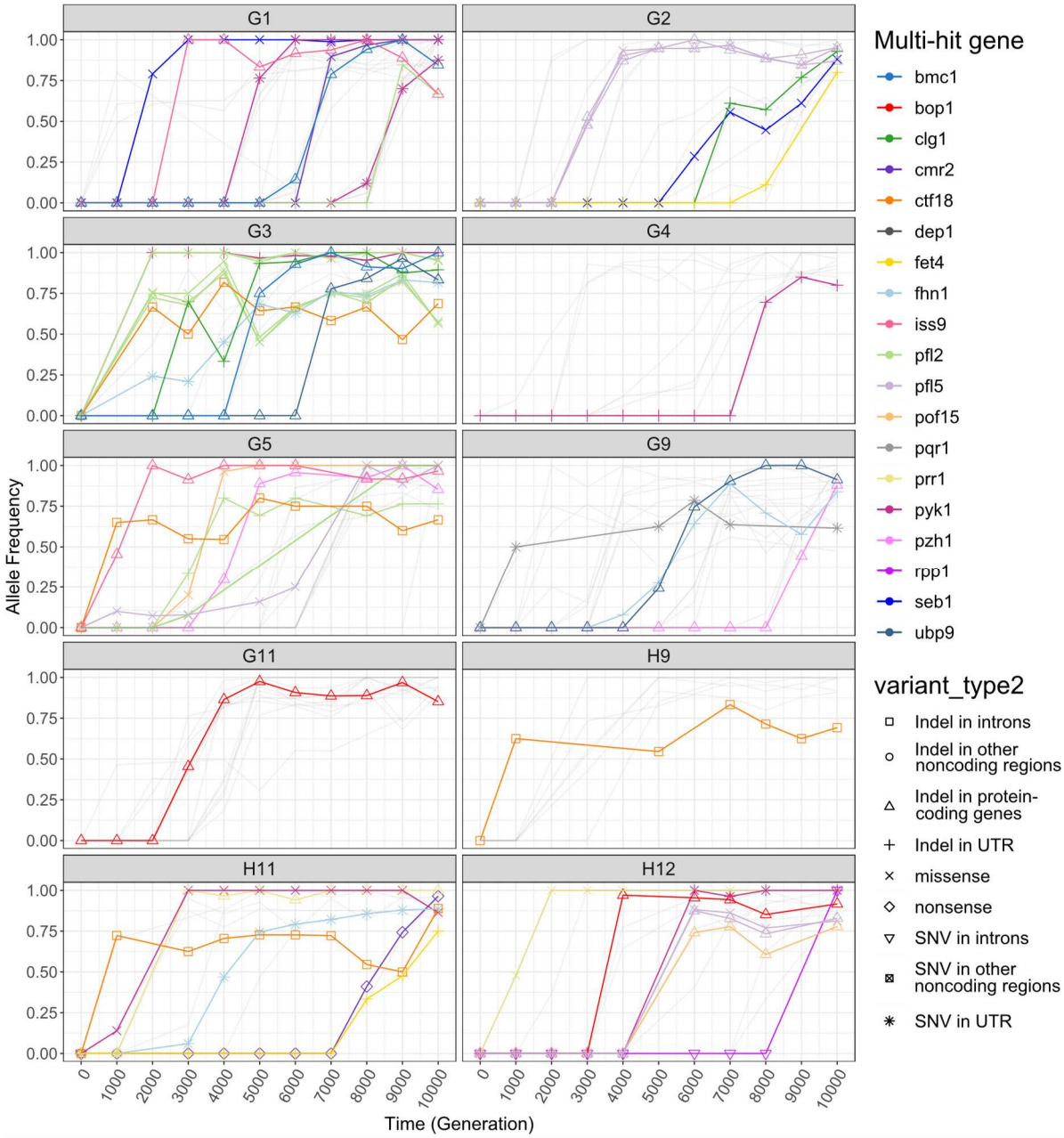

Figure 3 Time series of the hits' allele frequencies in evolved *S. pombe* populations and multi-hit genes. Time series of the hits' allele frequencies in the *S. pombe* populations. We defined a

"hit" as a fixed variant that is not synonymous (missense, nonsense and indels) and a multi-hit gene as a gene having hits in multiple populations. In each population, variants that were never fixed or that are not located in multi-hit genes are represented by more transparent lines.

We also found evidence for adaptation through LOF mutations in the 10 evolved *S. pombe* populations, although these mutations are primarily frameshift insertions rather than deletions. This is consistent with a different indel bias than in *S. cerevisiae*[3] (**Table 1; Figure 2**) and a preference for insertion, which we previously highlighted (**Supplementary Figure 2**).

Most of the *S. pombe* multi-hit genes are involved in the response to hypoxic stress (HS) and sometimes to oxidative stress (OS) (**Table 1**), which may be due to growth in an unshaken environment. Adapting to HS requires compensating for the energy deficit caused by respiration deficiency through fermentation and removing the associated reactive oxygen species (ROS)[30]. Further, the increase in ethanol production through fermentation can decrease lipid membrane integrity. This includes the mitochondrial membrane, which harbors the electron transport chain and antioxidant components that stabilize ROS through electron transfer. Thus, the increase in fermentation in hypoxic conditions can lead to ROS production through electron leakage[43]. This is consistent with fixed mutations in genes involved in the removal of damaged cell components and ROS like *clg1*, *bop1*, *pof15*, *pqr1*, *pzh1* and *ubp9*. Fermentation is also known to yield smaller energy and biomass outputs than respiration [30,32], which can affect the synthesis of redox metabolism components. Finally, *S. pombe* is known to be sensitive to polypeptones included in the growth media of the experiment (due to cell lysis), and it is thought that the respiratory Coenzyme Q (CoQ10) plays a role in promoting this trait[73,74]. Under the same conditions, *S. cerevisiae*, being petite-positive, can rely on fermentation along with a robust antioxidant response to mitigate the ROS produced by fermentation and hypoxic stress[43], which may explain why such mutations are not typically observed in budding yeast experimental evolution studies. Another piece of evidence supporting the importance of energy- and ROS-related processes in this environment is the fact that the strongest signal of convergent evolution is in the lower glycolysis gene *pyk1*, which had fixed mutations in 5 populations. This gene encodes for the enzyme involved in the synthesis of pyruvate, which influences respiration and fermentation as it can be transformed into Acetyl-CoA or into ethanol[33]. In the population H11, the glycolytic flux going towards respiration seems to be compromised by a fixed LOF mutation in *cmr2* (**Figure 3**), which encodes for the enzyme converting pyruvate into Acetyl-CoA. The fixation of this LOF mutation might be related to a benefit in re-orienting the glycolytic flux mostly towards fermentation. In the same population, we also observed the fixation of a LOF mutation in *prr1*, which encodes a transcription factor involved in the response to OS. Because *prr1* is not known to be directly activated by HS, there might be other OS response genes involved in ROS removal under HS, and *prr1* might not be needed unless ROS levels exceed the removal capabilities of these genes. For instance, in *S. pombe,* the transcription factor Sre1 is activated under low oxygen levels and activates genes involved in ROS removal or protein catabolism like *ccs1* and *SPAC23C11.06c*[61,75]. The benefit of inactivating *prr1* while respiration is limited under HS might thus be related to conserving energy and cell resources. However, losing such response regulators and relying on fermentation may lead *S. pombe* to be more sensitive to OS.

Evolved *S. pombe* populations are more sensitive to oxidative stress

As we observed fixed LOF mutations in genes modulating OS response and the glycolytic flux towards respiration, we hypothesized that evolved populations might be more sensitive to OS. Populations adapting to hypoxic stress or to polypeptone-mediated lysis may exhibit decreased respiration rates, resulting in reduced energy and biomass production[30]. This could affect the synthesis of the components of the redox metabolism, e.g. glutathione (GSH) and ubiquinone (CoQ10)[76,77]. These enzymes and the ones involved in the respiratory chain rely on the biomass produced by glycolysis and the TCA cycle as well as ions like iron and sulfur for their functions[30,76,78,79]. Consistent with this, we observed the presence of mutations in the iron transporter *fet4* in multiple populations, which may compensate for respiration deficiency. Indeed, iron can help capture or transport the low amount of oxygen available, and iron is a critical component of the respiratory chain enzymes. As previously mentioned, one *S. pombe* evolved population harbors a LOF insertion in *prr1* (**Table1**, **Figure 3**), an important transcription factor involved in the response to oxidative stress[70]. As *prr1* activates the catalase *ctt1*, the sulfiredoxin *srx1*, and the thioredoxin *trr1*[69], a fixed LOF mutation in this gene suggests that evolving under HS can decrease *S. pombe*'s ability to manage OS, which is consistent with observations in the cousin species *S. japonicus*[30]. These species likely rely on fermentation to adapt to hypoxic conditions, which may expose them to more ROS[43]. Altogether, these observations led us to believe that the evolved *S. pombe* populations are more sensitive to OS than WT as a result of their adaptation to HS.

To test this, we used hydrogen peroxide as a source of oxidative stress during a growth assay (**Methods**) and compared the OS sensitivity of the WT to the OS sensitivity of the 10 evolved populations (**Figure 4A**).

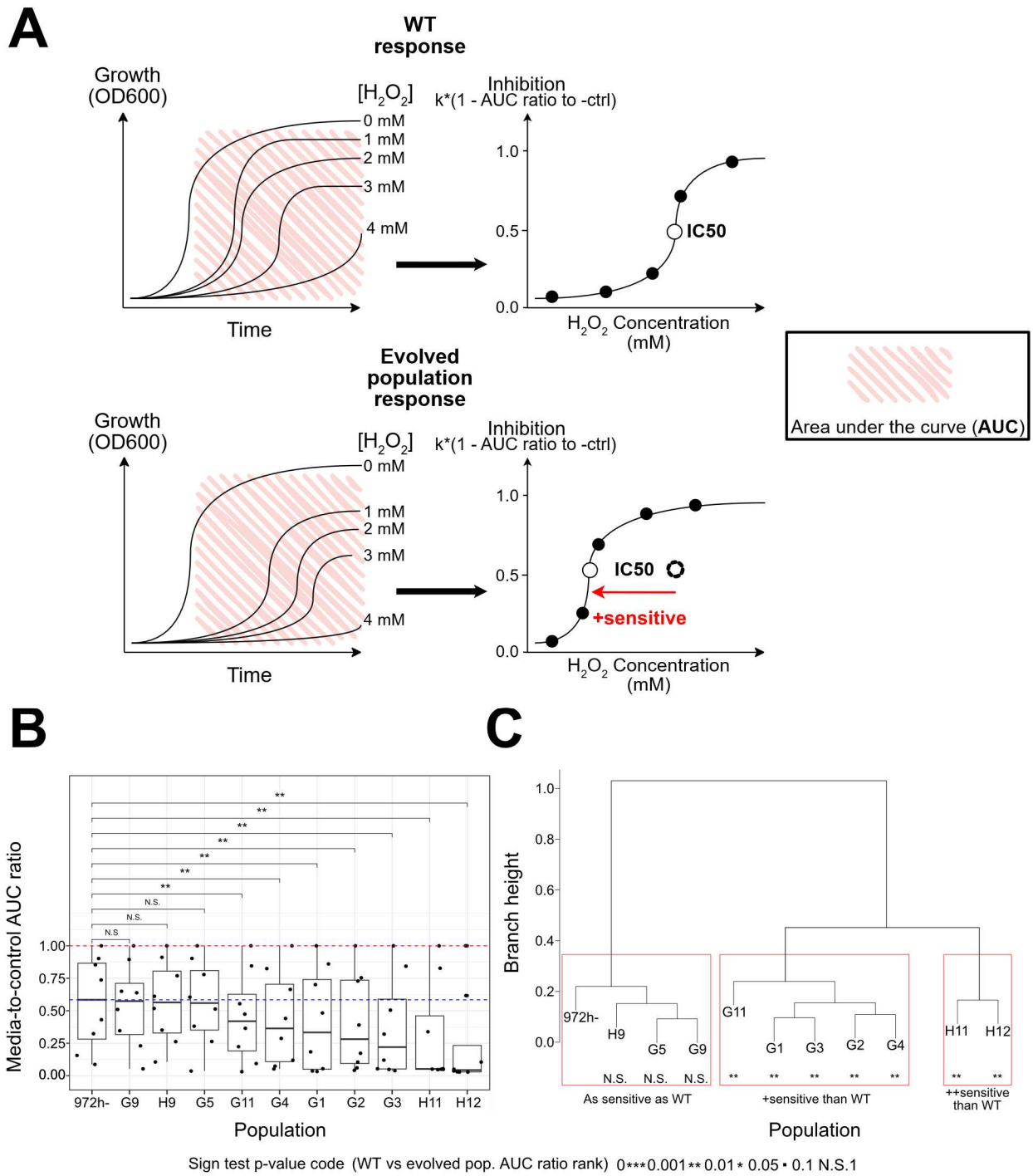

Figure 4 Comparison of the sensitivity levels to H_2O_2 between *S. pombe* WT and evolved populations. A) Schematic illustrating the expected difference in sensitivity between WT and evolved populations. We inferred the degree of inhibition at each concentration of H_2O_2 based on the expression in Equation 4 and the sensitivity of each population based on Dose-Response analysis (**Methods**). The IC50 recapitulates the level of sensitivity of a population to hydrogen peroxide. Lower IC50 values can be interpreted as higher sensitivity to H_2O_2, which is what we expected for the evolved populations. B) The ratio between the AUC of a population at a certain

H_2O_2 concentration + YPD and the AUC in YPD without H_2O_2. This is another metric of sensitivity with an expected maximum of 1 (red dotted line). The blue dotted line represents the median sensitivity of the WT. The WT AUC ratio is compared to each evolved population using a sign test on the ranks. The p-values of this test are encoded as follows: *** from 0 to 0.001 exclusively, ** from 0.001 to 0.01 exclusively, * from 0.01 to 0.05 exclusively, "." from 0.05 to 0.1 exclusively and N.S. otherwise, which is the acronym of "non-significant". C) Red boxes represent the population clusters, which are based on the AUC ratios.

The evolved populations clustered into 3 groups: 3 out of 10 populations had a similar sensitivity to H_2O_2 as the WT, 5 out of 10 populations were more sensitive than WT, and 2 out of 10 evolved populations were much more sensitive than the WT strain, including H11, the population that lost the OS response regulator *prr1* (**Figures 4B** and **4C**). This increased sensitivity to OS after adapting to HS has not been observed in *S. cerevisiae*, which may be explained by contingency, i.e. more exposure to anaerobic environments during its evolutionary history and a better redox metabolism[30,32]. However, it is reproducible in most of the evolved *S. pombe* populations, and has likewise been observed in related species, including wild *S. japonicus*[30] (see Discussion).

Transcriptomics analysis reveals many genes involved in the response to HS and downstream effects explaining the sensitivity to OS in multiple populations

The sensitivity to OS developed after adapting to HS was revealed by convergent evolution at the genomic level, i.e. multi-hit genes. However, identifying transcriptomic differences between more sensitive and WT-like populations could help reveal new genes involved in this trade-off and explain how point mutations and indels contribute to the evolution of these traits through transcriptomic regulation. Moreover, most of the mutations in the pyruvate kinase (*pyk1*) locus are located in the untranslated regions flanking the gene, which contains cis-regulatory elements (CRE) like the promoter (**Supplementary figure 5**). Hits in these loci could explain the adaptation to HS through changes in transcript levels through cis-regulatory and trans-regulatory effects[80–84]. These questions thus led us to investigate the role of transcriptomic changes in the responses to HS and OS.

Consistent with the need to compensate for biomass and energy deficit under HS due to limited respiration[30], most evolved *S. pombe* populations upregulated genes involved in heme metabolism/transport, the transport of biomolecules like amino acids or hexose, lipid metabolism, fermentation, and ion transport (**Figure 5, Supplementary Table 1**).

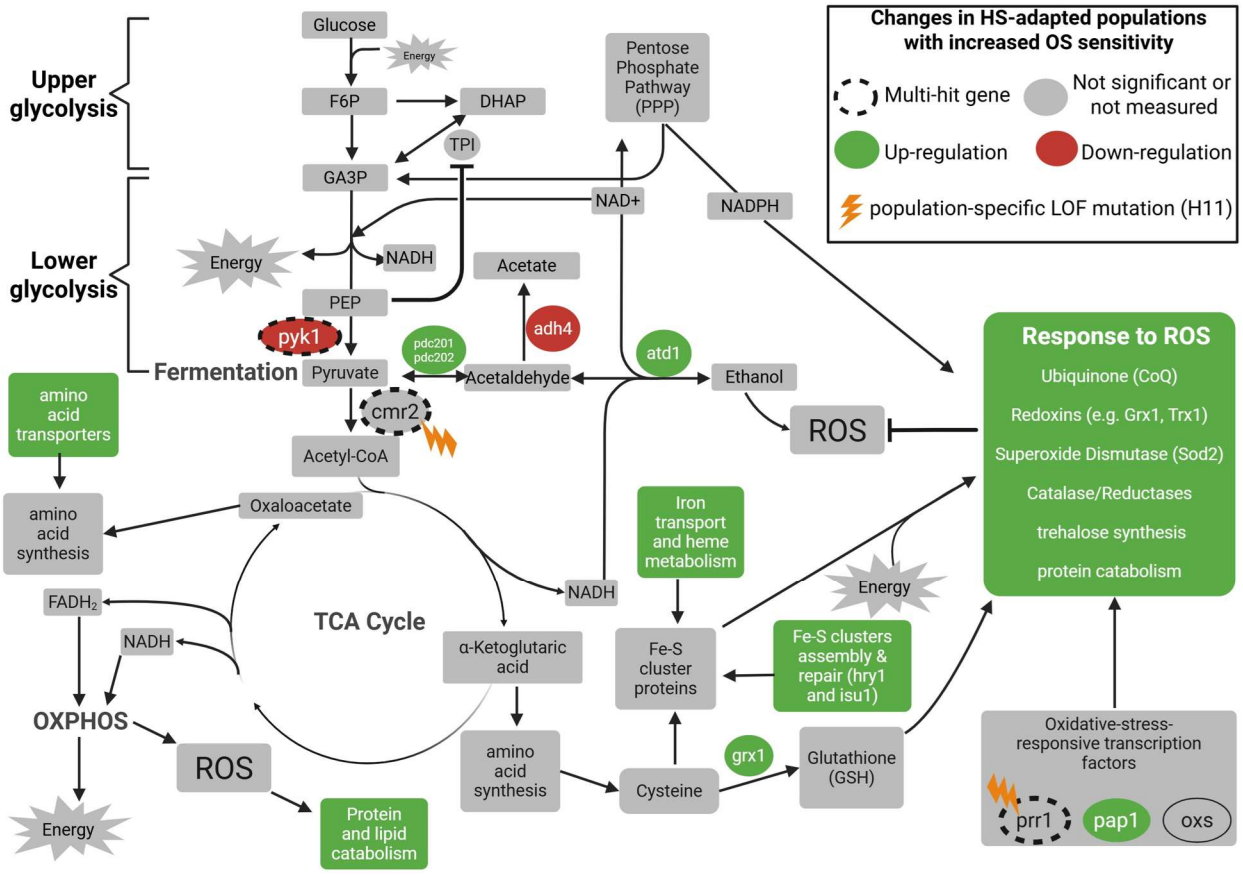

Figure 5 Fission yeast cellular responses to hypoxic stress in populations with increased OS sensitivity. Transcriptomic changes are determined by comparing the populations with increased OS sensitivity to populations with similar OS sensitivity than WT while genomic changes are obtained by comparing these evolved populations to WT (**Methods**). The green fill represents an upregulation while the red fill represents a downregulation. The grey fill represents molecules or processes that were not associated with a significant effect or not measured (no data). The orange lightning symbol represents LOF hits in H11, the only population with such variants in several multi-hit genes (dotted line stroke).

Another way the fission yeast populations could respond to HS is by improving the electron transport chain (ETC) to leverage the limited amount of oxygen available. The upregulation of the heme transporters *str3* and *shu1* in many evolved populations supports such a strategy (**Supplementary Table 1**). Heme can help capture and transport the small amount of oxygen available under HS and it is an essential component of the electron transport chain (ETC)[78].

Despite the presence of transcriptomic changes explaining HS adaptation and the OS sensitivity cost, most of the differentially expressed genes were different than the targets of selection identified at the genomic level, except for *pyk1*, *pzh1* and *ubp9*. For instance, the multi-hit gene *clg1*, which is a positive regulator of autophagy[38,60], is not differentially expressed between populations with different OS sensitivity, but 22 other genes involved in autophagy exhibit an expression level increase from 54.4% to 229% (**Supplementary Table 1**) and they are not mutated. Autophagy might be one of the few pathways that contribute to cross-resistance to both HS and OS by recycling biomolecules and removing damaged cell components[61,62]. Another

process linked to cross-resistance to multiple stresses is vesicular transport[85,86]. One of its genes, i.e. *ubp9,* is one of the only three multi-hit genes to be differentially expressed in evolved *S. pombe* populations that are more sensitive to OS than WT (log2FC = 0.885; FDR<0.05), suggesting a moderate but significant link between vesicular transport and adaptation (**Supplementary Table 1)**. As for the multi-hit gene *pyk1*, it is downregulated by 26.5% in populations with increased OS sensitivity (FDR<0.05). Adaptation to HS may require decreasing the glycolytic flux allocated to respiration[30] and change the respiration/fermentation balance. This is consistent with the decrease of Acetyl-CoA synthesis through the downregulation of the Acetyl-CoA ligase *pcs60* (53.7% decrease; FDR<0.05) and selected LOF mutations in *cmr2*, which may trigger the ETC optimization responses previously described as a compensatory mechanism. Similar to mutations observed in *S. japonicus*, the LOF mutations in lower glycolysis and Acetyl-CoA synthesis might also contribute to OS sensitivity in *S. pombe* as it would decrease the biomass and energy output of respiration, which is used for the synthesis of redox metabolism proteins[76,77]. The last differentially expressed multi-hit gene is *pzh1* (log2FC = 0.752; FDR<0.05), which regulates the activity of the plasma membrane H+-ATPase[87]. This is consistent with the need to increase energy production to compensate for respiration deficiency in hypoxic conditions.

Apart from these three multi-hit genes, transcriptomic changes shared by populations with increased OS sensitivity involved genes that were not mutated at the genomic level (**Supplementary Table 1; Table 1**). This is the case for many upregulated genes involved in fermentation, e.g. *pdc201/202* and *atd1*, and in the synthesis of ETC components and their iron-sulfur clusters, e.g. *cbp3-4, cbp6, coq9, sdh3, sdh8*, *qcr7-10*, *fxn1* and *isu1*. The lack of overlap between selection targets at the genomic and transcriptomic levels suggests that the changes in expression levels shared by many evolved populations are driven by trans-regulatory rather than by cis-regulatory effects.

DISCUSSION

Over short periods of time, experimental evolution is a powerful tool to decipher molecular pathways under selective constraints[3,11]. An important result from studies exploiting asexual laboratory evolution is that evolution is usually not limited by mutation: adaptation usually proceeds rapidly and is often dominated by large-effect mutations. In many cases, gene content variation can occur (via ploidy changes), and mutations frequently inactivate gene function. Perhaps the most interesting result from many of these studies is that laboratory evolution can frequently recapitulate evolutionary outcomes from wild, uncontrolled evolution. Whole-genome duplication, loss-of-function mutations, the rise of mutators, stable co-existence, and like here the change of carbon flow towards increased fermentation, are all phenomena thought to have occurred in various species at various times during the evolutionary history, but also notably in cancer cells[11,88–90]. Because cancer cells are also evolving populations, this suggests that experimental evolution in different single-cell organisms can reveal fundamental principles of the molecular basis of adaptation like the pervasiveness of parallel evolution in the tree of life due to deep conservation of interconnected biological pathways.

Our study extends the discovery of shared molecular mechanisms of adaptation at various scales in different biological systems. For instance, *S. pombe* shares a distinct preference for insertions as a mutational bias with *C. elegans*[38,]. On specific selection targets, mutations that lead to upregulation of iron metabolism, autophagy regulators and vesicle transporters, and that lead to

rewiring of the glycolytic flux are common observations in populations adapting under iron and oxygen limitation[92,93] (such as tumors). Finally, parallel evolution within model systems is frequent and observed in nearly all experimental evolution studies in various to date, but the precise observed trait under selection varies (examples in [6,94] and reviewed in[95]).

Despite all these common evolutionary mechanisms and outcomes, disparities can arise due to differences in genome architecture and contingency. One of the major findings in evolutionary dynamics is that low-fitness populations typically adapt faster than high-fitness populations. This observation has been seen in several species, and in several environmental contexts[3,6,11]. In the evolution environment of our study, the 'ancestor' *S. cerevisiae* is much fitter than its *S. pombe* counterpart. Yet, the fitness gains by our *S. pombe* populations are relatively modest (**Figure S1**). We propose that one explanation for this 'evolvability' is the effect that we set out to study in the first place, which is evolutionary contingency. Indeed, in a previous study, it was found that the identity of specific molecular pathways of gene deletions had a strong impact on fitness gain after evolution[13].

Further supporting this, the most frequent targets of adaptation in the past *S. cerevisiae* study were genes involved in adenine biosynthesis and the mating pathway; however, these pathways are not targets of selection in these *S. pombe* populations. Based on our understanding of the adenine biosynthetic pathways in both species, mutations in adenine biosynthesis genes were not expected in our *S. pombe* populations (which are ade+). In contrast, the *S. cerevisiae* populations were *ade2*-, which led them to accumulate a toxic intermediate that can be suppressed by the observed adenine pathway mutations after evolution. It is well known that similar effects can be observed in *ade6*- strains of *S. pombe*[96]. Similarly, mutations in the mating pathway might not be observed in *S. pombe* due to its preferential haploid lifestyle and its mating pathway is not active in rich media[21,22].

A third pathway frequently mutated in the budding yeast laboratory evolution experiment is the Ras-cAMP pathway[3,8,97]. Observed loss-of-function mutations in *IRA1* or *IRA2* (but usually not both), relieve inhibition of Ras and lead to PKA activation [3,98]. Activation of PKA ultimately leads to increased glycolysis through phosphorylation of Pyk1[99]. Our *S. pombe* populations never mutated the *IRA1/2* ortholog (*gap1*), though we note that it is a single-copy gene in the fission yeast. More surprisingly though, are the mutations observed in *pyk1*. These mutations are not the usual loss-of-function nonsense or frameshift mutations. Instead, most mutations were found in the regulatory region of the gene, which we initially believed to be an analogous way for *S. pombe* to upregulate Pyk1 activity. However, whole-transcriptome analyses suggest that these mutations downregulate Pyk1 activity (**Figure 5**). Interestingly, similar mutations leading to lower Pyk1 activity have been observed in wild *S. pombe* populations and in the common laboratory strain[33], suggesting that decreasing Pyk1 activity may be adaptive. In Kamrad et al. (2020), the authors showed that a decrease in Pyk1 activity does not increase growth rate nor biomass, seemingly contradicting the strong signature of adaptation from parallel evolution. However, the authors noted that lower Pyk1 activity might be an adaptive trade-off as lower glycolytic flux increases oxidative stress resistance through higher pentose-phosphate pathway flux and NADPH production. Despite transcriptomic analyses showing a slight decrease in Pyk1 expression levels

in most evolved *S. pombe* populations, they were often more sensitive to OS than WT. This is explained by the fact that during our experiment, the slightly reduced glycolytic flux is mostly redirected toward fermentation, which is upregulated to compensate for the fission yeast respiration deficiency in hypoxic conditions. This led to a trade-off of increased HS adaptation and OS sensitivity via multiple molecular mechanisms. First, Pyk1 activity can regulate carbon flow and, like the other mutations found in the wild, can favor fermentation rather than respiration, as our unshaking environment is likely to lead to hypoxic stress. Supporting this, we observed adaptations to HS, including LOF in enzymes responsible for the transition between glycolysis and OXPHOS, and the upregulation of the fermentation rate. This leads to an increase in intracellular ROS through higher ethanol production and a deficiency in the production of biomass and energy, which sustains the redox metabolism[32,43]. Second, *S. pombe* cells are sensitive to polypeptones, a major component of our environment[73]. Mutations that lower respiration and flux through the mitochondrial electron transport chain have been shown to increase resistance to polypeptones because this sensitivity requires CoQ10. Thus, the effects of reducing Pyk1 activity here is consistent with the other mutations we observed that appear to modulate central carbon metabolism (**Figures 3 and 5**). Strikingly, there is also evidence in *S. japonicus* that lower glycolysis is frequently being rewired in natural populations[30]. This suggests that adaptation to HS in petite-negative yeast species with relatively modest fermentation rates might come at the expense of costly carbon flow rewiring, hindering the response to OS.

Multiple genomic variants and transcriptomic changes were involved in the trade-off between HS and OS, e.g. LOF or downregulation in lower glycolysis or Acetyl-CoA synthesis, upregulation of fermentation, and upregulation of biomolecules and ions transport and metabolism. Among these adaptations to HS, fermentation upregulation and LOF in lower glycolysis and genes involved in the response to oxidative stress such as *prr1*, explain the increased sensitivity to OS. However, some genes involved in OS response, autophagy and vesicle transport may contribute to cross-resistance to both stresses[85,86,100–102]. This cross-resistance is also observed in other species like *K. lactis, S. cerevisiae* and human cancer[64,103–105]. In *S. pombe*, the effect of the cross-resistance pathways was not large enough to offset the cost of adapting to HS through the rewiring of the glycolytic flux toward fermentation and using the latter as the main source of biomass and energy despite its lower yield. The fact that this trade-off has not been observed in the budding yeast may be explained by its historical exposure to multiple anaerobic environments and more optimal adaptations to HS[32]. In contrast, *S. pombe* and *S. japonicus,* for which lower glycolysis is less active compared to *S. cerevisiae*, tend to adapt to HS through LOF in lower glycolysis and upregulation of fermentation and upper glycolysis[30,33]. Furthermore, the fact that the response to HS mostly involved transcriptomic changes in genes that were not mutated in coding or flanking regulatory regions suggests that the adaptive transcriptomic changes observed across populations were driven by trans-regulatory rather than cis-regulatory effects. This also shows that the transcriptome, which is an intermediate level of organization between genotype and phenotype, is a complex trait that can show evolutionary parallelism.

Despite the potential of these observations to improve evolutionary predictions, this study shows that various mechanisms are involved and that contingency leads to various evolutionary outcomes, even within a single species and under the same conditions. One way future research

could better predict adaptive trajectories under stress conditions is by leveraging the presence of rapid transcriptomic changes in response to a new stress independently of mutations, e.g. expression plasticity. These responses could provide hints toward adaptive cellular changes that could later be cemented by mutations with similar effects, as is the case in bird species that explore high-altitude conditions[11,106].

METHODS

Experimental evolution and sequencing

We evolved 15 *S. pombe* populations at 30°C in wells of a lidded, flat-bottom 96-well plate containing YPD for 10,000 generations, collecting and freezing samples at -80 °C every 70 generations. The remaining wells contained blank controls or populations of other yeast species and will be described elsewhere. This is the same procedure used to generate the compared *S. cerevisiae* dataset[3]. Because these conditions yield a doubling rate of 10 generations per day, we performed a 1/1024 serial dilution every day ($1/2^{10}$). This corresponds to an effective population size of ~6.00E04 and a bottleneck population size of ~8.00E03 [3,107]. We chose to perform whole-population whole-genome sequencing every 1,000 generations, and we were able to grow back cells from 93 out of these 100 samples after storage and sequenced these time points with Illumina NovaSeq paired-end sequencing (mean effective coverage ~40X). Raw DNA sequences are available on NCBI: https://www.ncbi.nlm.nih.gov/bioproject/PRJNA1315931.

Measuring fitness in the S. pombe populations

We grew the evolved populations, the WT, and a S. cerevisiae reference strain expressing GFP (YAN438: MATα, his3D1, ura3D0, leu2D0, lys2D0, can1::RPL39pr_ymGFP_Ste2pr-SpHIS5_Ste3pr_LEU2) for 24 hours. Next, because the green *S. cerevisiae* strain grew much faster than *S. pombe,* we prepared mixtures of the "dark" *S. pombe* populations and the green budding yeast at a 9:1 ratio and grew the mixed cultures for 24 hours. We then serially propagated each mixture for 3 days and used a Beckman-Coulter CytoFlex flow cytometer to measure the frequency of the "dark" *S. pombe* and the green *S. cerevisiae* strain daily. All particle counts were acquired at 30 µL/s rate for a maximum of 60 seconds or until 10,000 events were detected from a 96-well plate containing the mixtures. The data were analyzed using the CytoFlex acquisition and analysis software CytExpert. The "dark" *S. pombe* cells were distinguished from the green *S. cerevisiae* strain using FITC-A/PE-A gates. Using the cell counts, we then calculated the frequency of each population in the mixture and inferred fitness based on the slope of a linear regression between the logarithm of the frequency ratio and the number of generations:

$$\ln\left(\frac{frequency_{S.\ pombe}}{frequency_{green\ S.\ cerevisiae}}\right) = (Fitness * number\ of\ generations) + intercept \qquad \text{(Eq. 1)}$$

Variant calling

We used Varscan2.4.6[45] to call single-nucleotide variants (SNVs) and indels. Because contamination, sequencing errors and low-complexity regions can affect the variant calling, we applied some filters to the called variants. These filters ensure that the calls are supported by reads, are time-consistent, and are not affected by possible errors in the reference genome, e.g. avoiding confusion between ancestral alleles that were not present in the reference genome (972h-) and fixed de novo mutations. The variant calling pipeline is available at https://github.com/arnaud00013/Experimental_evolution_S_pombe.

Filter name	Criteria
Mapping quality	Mapping quality score ≥ 15 and eliminate indels in low-complexity regions (short tandem repeats or homopolymers)
Read bases quality	≥ Q20
Allele frequency	≥ 0.05
Reads containing the variant	≥5 reads in at least one strand and ≥2 reads in both strands
Contamination	Each read should best map to *S. pombe*
Evidence for sub-clonality and linkage disequilibrium	|Pearson r| ≥ 0.9 with at least one mutation from the same population
Variation in non-fixed variant allele frequency	≥ 0.1
Initial allele frequency	Eliminate variants with an allele frequency ≥ 0.4 in at least a third of the populations

Table 2 List of variant calling filters.

Identifying signatures of selection from the substitution spectrum

We defined substitutions as variants with an allele frequency >= 75%. Then, we compared the substitution spectrum of each population with the one expected after 10,000 generations of evolution under a neutral null model. The number of fixed variants in each mutation category is calculated based on the species' evolution rate, genome size, genome architecture (e.g. ratio of coding to non-coding regions in the genome), and the proportion of single-nucleotide mutations derived from the genetic code and associated with a specific category of mutations. This allowed to derive 2 equations:

$$Nb_subs_in_category_X_nm = S_{rate} * t * G_{size} * r_x * p_x \quad \text{(Eq. 2)}$$

$$Nb_indels_in_category_X_nm = I_{rate} * t * G_{size} * r_x \quad \text{(Eq. 3)}$$

where $Nb_subs_in_category_X_nm$ is the expected number of substitutions in a mutation category X assuming a neutral model of evolution, $Nb_indels_in_category_X_nm$ is the expected number of indels of type X assuming a neutral model of evolution, S_{rate} is the species substitution rate, I_{rate} is the species indel rate, t is the number of generations observed since the

start of the experiment, G_{size} is the species genome size, r_x is the proportion of the genome covered by protein-coding or non-coding sites, depending on the mutation category X and p_x is the proportion of single-nucleotide mutations derived from the genetic code that can be classified as mutations from category X.

Evaluating and comparing the sensitivity to hydrogen peroxide

We grew the 10 evolved *S. pombe* populations and the WT ancestor in the rows of a 96-well plate at 30°C for 36 hours. The media was YPD + hydrogen peroxide with H_2O_2 concentrations of 0 mM, 0.5 mM, 1 mM, 1.5 mM, 2 mM, 2.5 mM, 3 mM and 3.5 mM. Each row of the 96-well plate corresponded to a different concentration of H_2O_2. The growth of each population was estimated using the OD600 time series measured from a BioTek Synergy HTX plate reader. For each time series, the area under the curve (AUC) was measured using the R package growthcurver[108]. Using the AUC as a proxy for growth, we then compared the AUC of each population at different H_2O_2 concentrations to the AUC obtained when H_2O_2 is absent from the media. Next, we inferred the degree of inhibition with:

$$Inhibition = k * \frac{AUC_{media}}{AUC_{control}} \quad \text{(Eq. 4)}$$

where k is a normalizing factor that makes sure the inhibition metric maximum is 1, AUC is the area under the growth curve, AUC_{media} represents the growth at a certain concentration of hydrogen peroxide and $AUC_{control}$ represents the growth in a YPD media without hydrogen peroxide. This expression is negatively correlated to the AUC ratio and ranges from 0 to 1. Using the Dose-Response Analysis R package drc[109], we then fitted a log-logistic model to this metric and H_2O_2 concentrations to estimate the IC50, which recapitulates the level of sensitivity of a population to hydrogen peroxide.

RNA extraction, sequencing and transcriptomic analysis

We extracted in replicates the RNA of the evolved populations using an in-house protocol that works well with *S. cerevisiae*. Briefly, cells were grown to mid-log phase in YPD and lysed using 100 ul of 5 mg/mL Zymolyase + 10 mM DTT, incubated at 37° Celsius for 5 minutes. The weakened cells were then incubated with 100 ul of 2% SDS for a final SDS concentration of 1%. 200 ul of lysis buffer was added (4.5 M Guanidine thiocyanate, 10 mM EDTA) and mixed gently by inverting. The SDS was then precipitated using 200 ul of 3M Potassium acetate at pH 5.

After centrifugation, the lysate was passed through a minipreparation silica column to bind DNA. Under these conditions, RNA does not bind to the silica columns. Therefore, we collected the flowthrough. We then mixed it with an equal volume of pure isopropanol and passed it through another minipreparation silica column (which will now bind RNA). The column was then washed with 400 ul of wash buffer (10% Guanidine thiocyanate, 25% Isopropanol, and 10 mM EDTA), and then twice with 600 ul of 80% Ethanol. After drying the column, the RNA was eluted with 50 ul of 10 mM Tris pH 8.5. RNA integrity was verified on an agarose gel.

We sequenced the extracted RNA using NEBNext Ultra II on an Illumina NovaSeq X paired-end sequencing lane. This yielded 10.6E06 150-bp paired-end reads per sample on average (σ=1.32E06). Raw RNA-sequencing data are available on NCBI: https://www.ncbi.nlm.nih.gov/bioproject/PRJNA1315931. We pre-processed the reads with fastp (version 0.23.1) with the arguments --trim_poly_x --trim_poly_g --cut_front --cut_front_mean_quality 20 --cut_tail --cut_tail_mean_quality 20 --detect_adapter_for_pe[110]. Next, we mapped the reads to the reference (972h-) using samtools v1.17, removed duplicates with picard v2.26.3 and counted the number of reads per gene using featureCounts from subread v2.0.6[111–113]. Finally, we used the DESeq2 package to detect differentially expressed genes between populations that are as sensitive and more sensitive than WT[114]. The RNA-seq analysis pipeline is available at https://github.com/arnaud00013/Experimental_evolution_S_pombe.

REFERENCES

1. Kryazhimskiy, S., Rice, D. P., Jerison, E. R. & Desai, M. M. Microbial evolution. Global epistasis makes adaptation predictable despite sequence-level stochasticity. *Science* **344**, 1519–1522 (2014).
2. Couce, A. & Tenaillon, O. A. The rule of declining adaptability in microbial evolution experiments. *Front Genet* **6**, 99 (2015).
3. Johnson, M. S. *et al.* Phenotypic and molecular evolution across 10,000 generations in laboratory budding yeast populations. *eLife* **10**, e63910 (2021).
4. Good, B. H., McDonald, M. J., Barrick, J. E., Lenski, R. E. & Desai, M. M. The dynamics of molecular evolution over 60,000 generations. *Nature* **551**, 45–50 (2017).
5. Kinnersley, M. *et al.* Ex Uno Plures: Clonal Reinforcement Drives Evolution of a Simple Microbial Community. *PLOS Genetics* **10**, e1004430 (2014).
6. Tenaillon, O. *et al.* Tempo and mode of genome evolution in a 50,000-generation experiment. *Nature* **536**, 165–170 (2016).
7. Lang, G. I. *et al.* Pervasive genetic hitchhiking and clonal interference in forty evolving yeast populations. *Nature* **500**, 571–574 (2013).
8. Venkataram, S. *et al.* Development of a Comprehensive Genotype-to-Fitness Map of Adaptation-Driving Mutations in Yeast. *Cell* **166**, 1585-1596.e22 (2016).
9. Jerison, E. R. *et al.* Genetic variation in adaptability and pleiotropy in budding yeast. *eLife* **6**, e27167.
10. Burke, M. K. *et al.* Genome-wide analysis of a long-term evolution experiment with Drosophila. *Nature* **467**, 587–590 (2010).
11. Stroud, J. T. & Ratcliff, W. C. Long-term studies provide unique insights into evolution. *Nature* **639**, 589–601 (2025).

12. Bakerlee, C. W., Ba, A. N. N., Shulgina, Y., Echenique, J. I. R. & Desai, M. M. Idiosyncratic epistasis leads to global fitness-correlated trends. *Science* **376**, 630–635 (2022).
13. Echenique, J. I. R., Kryazhimskiy, S., Ba, A. N. N. & Desai, M. M. Modular epistasis and the compensatory evolution of gene deletion mutants. *PLOS Genetics* **15**, e1007958 (2019).
14. Helsen, J. *et al.* Gene Loss Predictably Drives Evolutionary Adaptation. *Molecular Biology and Evolution* **37**, 2989–3002 (2020).
15. Teng, X. *et al.* Genome-wide consequences of deleting any single gene. *Mol Cell* **52**, 485–494 (2013).
16. Galardini, M. *et al.* The impact of the genetic background on gene deletion phenotypes in Saccharomyces cerevisiae. *Mol Syst Biol* **15**, e8831 (2019).
17. Blount, Z. D., Borland, C. Z. & Lenski, R. E. Historical contingency and the evolution of a key innovation in an experimental population of Escherichia coli. *Proc Natl Acad Sci U S A* **105**, 7899–7906 (2008).
18. Huang, M.-E., Rio, A.-G., Nicolas, A. & Kolodner, R. D. A genomewide screen in Saccharomyces cerevisiae for genes that suppress the accumulation of mutations. *Proceedings of the National Academy of Sciences* **100**, 11529–11534 (2003).
19. Opulente, D. A. *et al.* Genomic factors shape carbon and nitrogen metabolic niche breadth across Saccharomycotina yeasts. *Science* **384**, eadj4503 (2024).
20. Shen, X.-X. *et al.* Tempo and Mode of Genome Evolution in the Budding Yeast Subphylum. *Cell* **175**, 1533-1545.e20 (2018).
21. Forsburg, S. L. Overview of. *Current Protocols in Molecular Biology* **64**, 13.14.1-13.14.3 (2003).

22. Vyas, A., Freitas, A. V., Ralston, Z. A. & Tang, Z. Fission Yeast Schizosaccharomyces pombe: A Unicellular “Micromammal” Model Organism. *Curr Protoc* **1**, e151 (2021).
23. Ward, C. M. *et al.* Recombination, admixture and genome instability shape the genomic landscape of Saccharomyces cerevisiae derived from spontaneous grape ferments. *PLoS Genet* **20**, e1011223 (2024).
24. Peter, J. *et al.* Genome evolution across 1,011 Saccharomyces cerevisiae isolates. *Nature* **556**, 339–344 (2018).
25. Chen, V. *et al.* Evolution of haploid and diploid populations reveals common, strong, and variable pleiotropic effects in non-home environments. *eLife* **12**, e92899 (2023).
26. Shapira, R., Levy, T., Shaked, S., Fridman, E. & David, L. Extensive heterosis in growth of yeast hybrids is explained by a combination of genetic models. *Heredity (Edinb)* **113**, 316–326 (2014).
27. Shapira, R. & David, L. Genes with a Combination of Over-Dominant and Epistatic Effects Underlie Heterosis in Growth of Saccharomyces cerevisiae at High Temperature. *Front Genet* **7**, 72 (2016).
28. Conant, G. C. & Wolfe, K. H. Increased glycolytic flux as an outcome of whole-genome duplication in yeast. *Mol Syst Biol* **3**, 129 (2007).
29. Vowinckel, J. *et al.* The metabolic growth limitations of petite cells lacking the mitochondrial genome. *Nat Metab* **3**, 1521–1535 (2021).
30. Alam, S., Gu, Y., Reichert, P., Bähler, J. & Oliferenko, S. Optimization of energy production and central carbon metabolism in a non-respiring eukaryote. *Current Biology* **33**, 2175-2186.e5 (2023).

31. Chen, X. J. & Clark-Walker, G. D. The petite mutation in yeasts: 50 years on. *Int Rev Cytol* **194**, 197–238 (2000).
32. Dashko, S., Zhou, N., Compagno, C. & Piškur, J. Why, when, and how did yeast evolve alcoholic fermentation? *FEMS Yeast Res* **14**, 826–832 (2014).
33. Kamrad, S. *et al.* Pyruvate kinase variant of fission yeast tunes carbon metabolism, cell regulation, growth and stress resistance. *Mol Syst Biol* **16**, e9270 (2020).
34. Bergström, A. *et al.* A High-Definition View of Functional Genetic Variation from Natural Yeast Genomes. *Molecular Biology and Evolution* **31**, 872–888 (2014).
35. Farlow, A. *et al.* The Spontaneous Mutation Rate in the Fission Yeast Schizosaccharomyces pombe. *Genetics* **201**, 737–744 (2015).
36. Wood, V. *et al.* The genome sequence of Schizosaccharomyces pombe. *Nature* **415**, 871–880 (2002).
37. Blevins, W. R. *et al.* Uncovering de novo gene birth in yeast using deep transcriptomics. *Nat Commun* **12**, 604 (2021).
38. Harris, M. A. *et al.* Fission stories: using PomBase to understand Schizosaccharomyces pombe biology. *Genetics* **220**, iyab222 (2022).
39. Behringer, M. G. & Hall, D. W. Genome-Wide Estimates of Mutation Rates and Spectrum in Schizosaccharomyces pombe Indicate CpG Sites are Highly Mutagenic Despite the Absence of DNA Methylation. *G3 (Bethesda)* **6**, 149–160 (2015).
40. Schlackow, M. & Gullerova, M. Understanding non-coding DNA regions in yeast. *Biochemical Society Transactions* **41**, 1654–1659 (2013).
41. Ohsawa, S. *et al.* Nitrogen signaling factor triggers a respiration-like gene expression program in fission yeast. *The EMBO Journal* **43**, 4604–4624 (2024).

42. Vassiliadis, D., Wong, K. H., Andrianopoulos, A. & Monahan, B. J. A genome-wide analysis of carbon catabolite repression in Schizosaccharomyces pombe. *BMC Genomics* **20**, 251 (2019).

43. Landolfo, S., Politi, H., Angelozzi, D. & Mannazzu, I. ROS accumulation and oxidative damage to cell structures in *Saccharomyces cerevisiae* wine strains during fermentation of high-sugar-containing medium. *Biochimica et Biophysica Acta (BBA) - General Subjects* **1780**, 892–898 (2008).

44. Synnott, J. M., Guida, A., Mulhern-Haughey, S., Higgins, D. G. & Butler, G. Regulation of the Hypoxic Response in Candida albicans. *Eukaryot Cell* **9**, 1734–1746 (2010).

45. Koboldt, D. C. *et al.* VarScan 2: somatic mutation and copy number alteration discovery in cancer by exome sequencing. *Genome Res* **22**, 568–76 (2012).

46. Koboldt, D. C. Best practices for variant calling in clinical sequencing. *Genome Medicine* **12**, 91 (2020).

47. Li, H. Toward better understanding of artifacts in variant calling from high-coverage samples. *Bioinformatics* **30**, 2843–2851 (2014).

48. Zhu, Y. O., Siegal, M. L., Hall, D. W. & Petrov, D. A. Precise estimates of mutation rate and spectrum in yeast. *Proceedings of the National Academy of Sciences of the United States of America* **111**, E2310 (2014).

49. Lynch, M. *et al.* A genome-wide view of the spectrum of spontaneous mutations in yeast. *Proceedings of the National Academy of Sciences of the United States of America* **105**, 9272 (2008).

50. Schacherer, J., Shapiro, J. A., Ruderfer, D. M. & Kruglyak, L. Comprehensive polymorphism survey elucidates population structure of S. cerevisiae. *Nature* **458**, 342–345 (2009).

51. Gallone, B. *et al.* Origins, evolution, domestication and diversity of *Saccharomyces* beer yeasts. *Current Opinion in Biotechnology* **49**, 148–155 (2018).

52. Duan, S.-F. *et al.* The origin and adaptive evolution of domesticated populations of yeast from Far East Asia. *Nat Commun* **9**, 2690 (2018).

53. Chen, H., Blum, J. E., Thalacker-Mercer, A. & Gu, Z. Impact of the Whole Genome Duplication Event on PYK Activity and Effects of a PYK1 Mutation on Metabolism in S. cerevisiae. *Front Mol Biosci* **8**, 656461 (2021).

54. Frost, A. *et al.* Comparing S. pombe and S. cerevisiae Genetic Interactions Reveals Functional Repurposing and Identifies New Organelle Homeostasis and Mitosis Control Genes. *Cell* **149**, 1339 (2012).

55. Aslett, M. & Wood, V. Gene Ontology annotation status of the fission yeast genome: preliminary coverage approaches 100%. *Yeast* **23**, 913–919 (2006).

56. Khan, T., Douglas, G. M., Patel, P., Nguyen Ba, A. N. & Moses, A. M. Polymorphism Analysis Reveals Reduced Negative Selection and Elevated Rate of Insertions and Deletions in Intrinsically Disordered Protein Regions. *Genome Biology and Evolution* **7**, 1815–1826 (2015).

57. Dupré, S., Urban-Grimal, D. & Haguenauer-Tsapis, R. Ubiquitin and endocytic internalization in yeast and animal cells. *Biochimica et Biophysica Acta (BBA) - Molecular Cell Research* **1695**, 89–111 (2004).

58. Zattas, D. & Hochstrasser, M. Ubiquitin-dependent Protein Degradation at the Yeast Endoplasmic Reticulum and Nuclear Envelope. *Crit Rev Biochem Mol Biol* **50**, 1–17 (2015).

59. Ryan, C. J. *et al.* Hierarchical Modularity and the Evolution of Genetic Interactomes across Species. *Molecular Cell* **46**, 691–704 (2012).

60. Matsuda, S., Kikkawa, U., Uda, H. & Nakashima, A. The S. pombe CDK5 ortholog Pef1 regulates sexual differentiation through control of the TORC1 pathway and autophagy. *Journal of Cell Science* **133**, jcs247817 (2020).

61. Todd, B. L., Stewart, E. V., Burg, J. S., Hughes, A. L. & Espenshade, P. J. Sterol Regulatory Element Binding Protein Is a Principal Regulator of Anaerobic Gene Expression in Fission Yeast. *Mol Cell Biol* **26**, 2817–2831 (2006).

62. Farrugia, G. & Balzan, R. Oxidative Stress and Programmed Cell Death in Yeast. *Front. Oncol.* **2**, (2012).

63. Rodríguez-López, M. *et al.* Broad functional profiling of fission yeast proteins using phenomics and machine learning. *eLife* **12**, RP88229 (2023).

64. Blanco, M. *et al.* An approach to the hypoxic and oxidative stress responses in Kluyveromyces lactis by analysis of mRNA levels. *FEMS Yeast Research* **7**, 702–714 (2007).

65. Rubio, A., Ghosh, S., Mülleder, M., Ralser, M. & Mata, J. Ribosome profiling reveals ribosome stalling on tryptophan codons and ribosome queuing upon oxidative stress in fission yeast. *Nucleic Acids Research* **49**, 383–399 (2021).

66. Kwon, E.-J. G. *et al.* Deciphering the Transcriptional-Regulatory Network of Flocculation in Schizosaccharomyces pombe. *PLoS Genet* **8**, e1003104 (2012).

67. Stewart, G. G. Yeast Flocculation—Sedimentation and Flotation. *Fermentation* **4**, 28 (2018).

68. Chen, D. *et al.* Global Transcriptional Responses of Fission Yeast to Environmental Stress. *Mol Biol Cell* **14**, 214–229 (2003).

69. Calvo, I. A., García, P., Ayté, J. & Hidalgo, E. The transcription factors Pap1 and Prr1 collaborate to activate antioxidant, but not drug tolerance, genes in response to H2O2. *Nucleic Acids Res* **40**, 4816–4824 (2012).

70. Quinn, J. *et al.* Two-Component Mediated Peroxide Sensing and Signal Transduction in Fission Yeast. *Antioxidants & Redox Signaling* **15**, 153–165 (2011).

71. Leiter, É. *et al.* Protein phosphatase Z modulates oxidative stress response in fungi. *Fungal Genet Biol* **49**, 708–716 (2012).

72. Kimura, M. Evolutionary rate at the molecular level. *Nature* **217**, 624–626 (1968).

73. Matsuo, Y. *et al.* Polypeptone Induces Dramatic Cell Lysis in ura4 Deletion Mutants of Fission Yeast. *PLOS ONE* **8**, e59887 (2013).

74. Kosugi, M. *et al.* Stereochemical assignment of the unique electron acceptor 5'-hydroxyphylloquinone, a polar analog of vitamin K1 in photosystem I. *Biosci Biotechnol Biochem* **81**, 2244–2252 (2017).

75. Hughes, A. L., Todd, B. L. & Espenshade, P. J. SREBP pathway responds to sterols and functions as an oxygen sensor in fission yeast. *Cell* **120**, 831–842 (2005).

76. Miki, R., Saiki, R., Ozoe, Y. & Kawamukai, M. Comparison of a coq7 deletion mutant with other respiration-defective mutants in fission yeast. *The FEBS Journal* **275**, 5309–5324 (2008).

77. Kaino, T., Tonoko, K., Mochizuki, S., Takashima, Y. & Kawamukai, M. Schizosaccharomyces japonicus has low levels of CoQ10 synthesis, respiration deficiency, and efficient ethanol production. *Bioscience, Biotechnology, and Biochemistry* **82**, 1031–1042 (2018).

78. Pluskal, T., Sajiki, K., Becker, J., Takeda, K. & Yanagida, M. Diverse fission yeast genes required for responding to oxidative and metal stress: Comparative analysis of glutathione-related and other defense gene deletions. *Genes to Cells* **21**, 530–542 (2016).

79. Uchida, N. *et al.* Phenotypes of Fission Yeast Defective in Ubiquinone Production Due to Disruption of the Gene for p-Hydroxybenzoate Polyprenyl Diphosphate Transferase. *J Bacteriol* **182**, 6933–6939 (2000).

80. Wittkopp, P. J., Haerum, B. K. & Clark, A. G. Evolutionary changes in cis and trans gene regulation. *Nature* **430**, 85–88 (2004).

81. Wittkopp, P. J. & Kalay, G. Cis-regulatory elements: molecular mechanisms and evolutionary processes underlying divergence. *Nat Rev Genet* **13**, 59–69 (2011).

82. Liu, X., Li, Y. I. & Pritchard, J. K. Trans Effects on Gene Expression Can Drive Omnigenic Inheritance. *Cell* **177**, 1022-1034.e6 (2019).

83. Yao, C. *et al.* Dynamic Role of trans Regulation of Gene Expression in Relation to Complex Traits. *Am J Hum Genet* **100**, 571–580 (2017).

84. Renganaath, K. & Albert, F. W. Trans-eQTL hotspots shape complex traits by modulating cellular states. *bioRxiv* 2023.11.14.567054 (2024) doi:10.1101/2023.11.14.567054.

85. Zakrzewska, A. *et al.* Genome-wide analysis of yeast stress survival and tolerance acquisition to analyze the central trade-off between growth rate and cellular robustness. *Mol Biol Cell* **22**, 4435–4446 (2011).

86. Alejandro-Osorio, A. L. *et al.* The histone deacetylase Rpd3p is required for transient changes in genomic expression in response to stress. *Genome Biol* **10**, R57 (2009).

87. Balcells, L. *et al.* The Pzh1 protein phosphatase and the Spm1 protein kinase are involved in the regulation of the plasma membrane H+-ATPase in fission yeast. *FEBS Letters* **435**, 241–244 (1998).

88. Shahrouzi, P., Forouz, F., Mathelier, A., Kristensen, V. N. & Duijf, P. H. G. Copy number alterations: a catastrophic orchestration of the breast cancer genome. *Trends in Molecular Medicine* **30**, 750–764 (2024).

89. Al Tameemi, W., Dale, T. P., Al-Jumaily, R. M. K. & Forsyth, N. R. Hypoxia-Modified Cancer Cell Metabolism. *Front. Cell Dev. Biol.* **7**, (2019).

90. Steele, C. D. *et al.* Signatures of copy number alterations in human cancer. *Nature* **606**, 984–991 (2022).

91. Denver, D. R., Morris, K., Lynch, M. & Thomas, W. K. High mutation rate and predominance of insertions in the Caenorhabditis elegans nuclear genome. *Nature* **430**, 679–682 (2004).

92. Jensen, L. T. & Culotta, V. C. Regulation of *Saccharomyces cerevisiae FET4* by Oxygen and Iron. *Journal of Molecular Biology* **318**, 251–260 (2002).

93. Daskalaki, I., Gkikas, I. & Tavernarakis, N. Hypoxia and Selective Autophagy in Cancer Development and Therapy. *Front Cell Dev Biol* **6**, 104 (2018).

94. Slomka, S. *et al.* Experimental Evolution of Bacillus subtilis Reveals the Evolutionary Dynamics of Horizontal Gene Transfer and Suggests Adaptive and Neutral Effects. *Genetics* **216**, 543–558 (2020).

95. McDonald, M. J. Microbial Experimental Evolution - a proving ground for evolutionary theory and a tool for discovery. *EMBO Rep* **20**, e46992 (2019).

96. Chaudhuri, B., Ingavale, S. & Bachhawat, A. K. Apd1(+), a Gene Required for Red Pigment Formation in Ade6 Mutants of Schizosaccharomyces Pombe, Encodes an Enzyme Required for Glutathione Biosynthesis: A Role for Glutathione and a Glutathione-Conjugate Pump. *Genetics* **145**, 75–83 (1997).

97. Li, Y. *et al.* Hidden Complexity of Yeast Adaptation under Simple Evolutionary Conditions. *Current Biology* **28**, 515-525.e6 (2018).

98. Williamson, T., Adiamah, D., Schwartz, J.-M. & Stateva, L. Exploring the genetic control of glycolytic oscillations in Saccharomyces Cerevisiae. *BMC Systems Biology* **6**, 108 (2012).

99. Cytryńska, M., Frajnt, M. & Jakubowicz, T. Saccharomyces cerevisiae pyruvate kinase Pyk1 is PKA phosphorylation substrate in vitro. *FEMS Microbiology Letters* **203**, 223–227 (2001).

100. Yu, Z.-Q. *et al.* Atg38-Atg8 interaction in fission yeast establishes a positive feedback loop to promote autophagy. *Autophagy* **16**, 2036–2051 (2020).

101. Zhao, D. *et al.* Atg20- and Atg24-family proteins promote organelle autophagy in fission yeast. *J Cell Sci* **129**, 4289–4304 (2016).

102. Su, Y., Chen, C., Huang, L., Yan, J. & Huang, Y. Schizosaccharomyces pombe Homologs of Human DJ-1 Are Stationary Phase-Associated Proteins That Are Involved in Autophagy and Oxidative Stress Resistance. *PLOS ONE* **10**, e0143888 (2015).

103. Liu, J. & Barrientos, A. Transcriptional Regulation of Yeast Oxidative Phosphorylation Hypoxic Genes by Oxidative Stress. *Antioxidants & Redox Signaling* **19**, 1916–1927 (2013).

104. Liu, J. & Wang, Z. Increased Oxidative Stress as a Selective Anticancer Therapy. *Oxid Med Cell Longev* **2015**, 294303 (2015).

105. Mendoza, E. N., Ciriolo, M. R. & Ciccarone, F. Hypoxia-Induced Reactive Oxygen Species: Their Role in Cancer Resistance and Emerging Therapies to Overcome It. *Antioxidants* **14**, 94 (2025).

106. She, H. *et al.* Gene expression plasticity followed by genetic change during colonization a high-elevation environment. *eLife* **12**, (2023).

107. Wahl, L. M. & Gerrish, P. J. The probability that beneficial mutations are lost in populations with periodic bottlenecks. *Evolution* **55**, 2606–2610 (2001).

108. Sprouffske, K. & Wagner, A. Growthcurver: an R package for obtaining interpretable metrics from microbial growth curves. *BMC Bioinformatics* **17**, 172 (2016).

109. Ritz, C., Baty, F., Streibig, J. C. & Gerhard, D. Dose-Response Analysis Using R. *PLOS ONE* **10**, e0146021 (2015).

110. Chen, S., Zhou, Y., Chen, Y. & Gu, J. fastp: an ultra-fast all-in-one FASTQ preprocessor. *Bioinformatics* **34**, i884–i890 (2018).

111. Li, H. *et al.* The Sequence Alignment/Map format and SAMtools. *Bioinformatics* **25**, 2078–2079 (2009).

112. Picard toolkit. *Broad Institute, GitHub repository* (2019).

113. Liao, Y., Smyth, G. K. & Shi, W. featureCounts: an efficient general purpose program for assigning sequence reads to genomic features. *Bioinformatics* **30**, 923–930 (2014).

114. Love, M. I., Huber, W. & Anders, S. Moderated estimation of fold change and dispersion for RNA-seq data with DESeq2. *Genome Biol* **15**, 550 (2014).